Atmospheric
Chemistry
and Physics
Discussions

Open Access

Substantial secondary organic aerosol formation in a coniferous forest: observations of both day and night time chemistry

A. K. Y. Lee[1], J. P. D. Abbatt[1], W. R. Leaitch[2], S.-M. Li[2], S. J. Sjostedt[1,a], J. J. B. Wentzell[2], J. Liggio[2], and A. M. Macdonald[2]

[1]Department of Chemistry, University of Toronto, Toronto, Canada
[2]Science and Technology Branch, Environment Canada, Downsview, Canada
[a]now at: NOAA ESRL Chemical Sciences Division, Boulder, USA

Correspondence to: A. K. Y. Lee (klee@chem.utoronto.ca)

Abstract

Substantial biogenic secondary organic aerosol (BSOA) formation was investigated in a coniferous forest mountain region at Whistler, British Columbia. A largely biogenic aerosol growth episode was observed, providing a unique opportunity to investigate BSOA formation chemistry in a forested environment with limited influence from anthropogenic emissions. Positive matrix factorization of aerosol mass spectrometry (AMS) measurement identified two types of BSOA (BSOA-1 and BSOA-2), which were primarily generated by gas-phase oxidation of monoterpenes and perhaps sesquiterpenes. The temporal variations of BSOA-1 and BSOA-2 can be explained by gas-particle partitioning in response to ambient temperature and the relative importance of different oxidation mechanisms between day and night. While BSOA-1 will arise from gas-phase ozonolysis and nitrate radical chemistry at night, BSOA-2 is less volatile than BSOA-1 and consists of products formed via gas-phase oxidation by the OH radical and ozone during the day. Organic nitrates produced through nitrate radical chemistry can account for 22–33 % of BSOA-1 mass at night. The mass spectra of BSOA-1 and BSOA-2 have higher values of the mass fraction of m/z 91 (f91) compared to the background organic aerosol, and so f91 is used as an indicator of BSOA formation pathways. A comparison between laboratory studies in the literature and our field observations highlights the potential importance of gas-phase formation chemistry of BSOA-2 type materials that may not be captured in smog chamber experiments, perhaps due to the wall loss of gas-phase intermediate products.

1 Introduction

Biogenic secondary organic aerosol (BSOA) generated by gas-phase oxidation of biogenic volatile organic compounds (BVOCs, such as isoprene, monoterpenes, and sesquiterpenes) emitted from vegetation is one of the major contributors to the global SOA budget (Hallquist et al., 2009). As a result of the atmospheric importance of

BSOA, many laboratory studies have focused on determining the mass yields and chemical characteristics of BSOA from oxidation of different gas-phase precursors (e.g., Chhabra et al., 2010; Lee et al., 2006a, b). However, chamber SOA is usually less oxidized than ambient SOA (e.g., Aiken et al., 2008; Ng et al., 2011), indicating that the current understanding of BSOA formation remains incomplete. Furthermore, the SOA yield parameters for atmospheric models and the degree of oxygenation of chamber SOA largely depends on the experimental conditions such as organic aerosol mass loading and seed particle surface area (Ehn et al., 2012; Shilling et al., 2009; Zhang et al., 2014).

Forested environments such as the boreal forest and Amazon rainforest can be considered giant chemical reactors for BSOA production (e.g., Chen et al., 2009; Ehn et al., 2012; Kanakidou et al., 2005; Slowik et al., 2010). Elevated temperature and/or solar radiation over forests can enhance their BVOCs emissions from the forest (Rinne et al., 2002; Leaitch et al., 2011), meanwhile BSOA can be produced efficiently due to active photochemistry during the day. Despite the fact that many field studies have been performed near or in forested areas to investigate BSOA formation, anthropogenic influence was frequently observed during those studies, further complicating the SOA formation chemistry (e.g., Han et al., 2014; Setyan et al., 2012). In particular, it has been hypothesized that the interactions of BVOCs with anthropogenic pollutants contributed to high aerosol loadings in the southeastern United States (Goldstein et al., 2009). Shilling et al. (2013) observed that the enhancement of SOA formation from isoprene was strongly related to the NO_x concentrations in Sacramento, California. Xu et al. (2015) recently reported that isoprene-derived SOA was directly mediated by sulfate, and NO_x was shown to enhance night time SOA formation via nitrate radical oxidation of monoterpenes in the southeastern United States.

In addition to the uncertainties of anthropogenic-biogenic interactions on BSOA formation, there is growing evidence of uncaptured BSOA formation chemistry in smog chamber experiments. For example, Ehn et al. (2014) recently showed that the wall effects of smog chambers can result in a substantial loss of highly oxygenated or-

ganic compounds with vapor pressures orders of magnitude lower than previously identified gas-phase oxidation products of BVOCs (i.e. referred to as extremely low volatility organic compound, ELVOC). Furthermore, Zhang et al. (2014) illustrated that the formation yields of toluene-derived SOA depend on the seed-to-chamber surface area ratio predominantly due to the loss of SOA-forming vapour to the chamber wall. The observed yield suppression likely extends to BSOA formation systems. Mueller et al. (2012) reported that cis-pinonic acid, one of the first generation products from α-pinene ozonolysis, experienced a significant wall loss in smog chambers. Such wall losses have not been adequately taken into consideration when aerosols yields were reported from earlier chamber studies. As a result, conducting a field measurement in a forested environment without significant influence of anthropogenic emissions and without the constraints of smog chamber walls is an attractive approach that can be used to re-evaluate our current knowledge of BSOA formation.

In this study, we deployed an Aerodyne high-resolution time-of-flight aerosol mass spectrometer (HR-ToF-AMS) to characterize ambient aerosol in a coniferous forest mountain region at Whistler, British Columbia from 15 June to 28 July 2010. Simultaneous measurements of gas-phase VOCs were made with a high resolution proton-transfer reaction mass spectrometer (PTR-ToF-MS). The measurement was part of the Whistler Aerosol and Cloud Study (WACS) 2010 campaign (Macdonald et al., 2015). The study duration covered a period when the forested region in Whistler experienced persistently high levels of nearly pure BSOA up to about $5\,\mu g\,m^{-3}$, providing a unique opportunity to investigate BSOA formation in a coniferous forest. This amount of SOA formation is considerably larger than that observed in pure isoprene-emission-dominated forests, such as in the Amazon (Martin et al., 2010). Rather, it matches the very high levels of BSOA observed in the summertime in another northern location in central Canada (Slowik et al., 2010).

Positive matrix factorization (PMF) analysis was performed to understand the types of organic aerosol that contributed to the total organic aerosol mass during this time. The relative importance of different oxidation chemistry (i.e. ozonolysis, OH radical

Substantial SOA formation in a coniferous forest

A. K. Y. Lee et al.

and nitrate radical oxidation) on BSOA formation between day and night are evaluated. Compared to previous laboratory studies, the mass spectral characteristics of the BSOA factors identified in the current study provide insight into the BSOA formation mechanisms that may not be captured in smog chamber experiments.

2 Experiment

2.1 Sampling location and period

The Whistler Aerosol and Cloud Study (WACS) was a large-scale field campaign conducted at Whistler, British Columbia from 15 June to 28 July 2010 (Macdonald et al., 2015). One of the two sampling sites on Whistler Mountain (Raven's Nest, see Fig. S1 in the Supplement) sits within a coniferous forest mountain area at an elevation of 1320 m a.s.l. In this paper, we focus on the observations at Raven's Nest from 1 to 19 July 2010, covering a large BSOA event that lasted approximately 5 days (6–10 July) and contrast them with those from a period with mixed biogenic and anthropogenic influence (13–18 July) (Figs. 1 and S2, and see Sect. 3 for discussion). Key measurements used in this analysis are briefly described in the following sections.

2.2 Aerosol measurements

An Aerodyne high-resolution time-of-flight aerosol mass spectrometer (HR-ToF-AMS, Aerodyne Research Inc.) and scanning mobility particle sizer (SMPS; TSI Inc., model 3936L75) were deployed to measure real-time non-refractory particulate matter (NR-PM, i.e., ammonium, nitrate, sulfate and organic) and particle number size distributions (16–685 nm), respectively. The ambient air was drawn through a stainless steel sampling line by the HR-ToF-AMS and other collocated particle instruments (Macdonald et al., 2015). The working principle of the HR-ToF-AMS has been reported in detail previously (DeCarlo et al., 2006). In brief, an aerodynamically focused particle beam impacts a tungsten vaporizer that was maintained at $\sim 600\,^\circ\text{C}$ to vaporize the NR-PM,

and the resulting vapors are ionized with electron impact ionization. The ions are then detected by a high-resolution time-of-flight mass spectrometer, which was operated in V-mode (5 min, mass resolving power ~ 2000 with a higher sensitivity) and W-mode (5 min, mass resolving power ~ 4000 with a lower sensitivity) alternatively. Ionization efficiency (IE) calibrations were performed on-site using monodisperse ammonium nitrate particles. The default relative IE (RIE) of nitrate, sulfate, ammonium, chloride and organic were used (Jimenez et al., 2003).

The data were processed using the AMS data analysis software (Squirrel, version 1.51H for unit mass resolution (UMR) data and Pika, version 1.10H for high resolution peak fitting, http://cires.colorado.edu/jimenez-group/ToFAMSResources/ToFSoftware/index.html) with the corrected air fragment column of the standard fragmentation table (Allan et al., 2004; DeCarlo et al., 2006). The data reported here are obtained from the high-resolution mass spectral fitting of W-mode data. Elemental analysis (oxygen- and hydrogen-to-carbon ratios, O : C and H : C) is based on the improved-method proposed by Canagaratna et al. (2015). Positive matrix factorization (PMF, PMF Evaluation Tool (PET) version 2.06) was used to analyze the AMS organic measurement for identification of the forms of organic aerosol in this study (Ulbrich et al., 2009).

2.3 VOC measurements

Measurements of volatile organic compounds (VOCs) were performed using a high-resolution proton transfer time-of-flight mass spectrometer (PTR-ToF-MS, Ionicon Analytik GmbH). The ambient air was drawn through a 5 m-long Perfluoroalkoxy (PFA) sampling line by a diaphragm pump at a rate of 5 standard L min^{-1}. A 200 sccm sample was drawn into the instrument through a heated inlet from the sampling line. Five-minute backgrounds were collected hourly through a platinum wool catalyst heated to 350 °C. The time resolution of measurement was 1 min. The raw PTR-ToF-MS data were acquired by the TofDaq software (Tofwerk AG, Switzerland) and post processed by PTR-MS ToF Viewer (Ionicon Analytik GmbH). Operations of proton transfer reaction mass spectrometer (PTR-MS) with a quadrupole mass spectrometer have been pre-

sented in great detail (Blake et al., 2009, de Gouw and Warneke, 2007). Briefly a PTR-MS is a soft ionization technique that allows for detection of VOCs that have a greater proton affinity than water. While the ionization process is the same in the PTR-ToF-MS as the PTR-MS, the high-resolution time-of-flight mass spectrometer used in the PTR-ToF-MS captures the entire mass spectrum from 12 to a high mass number (usually about 400) at high time resolutions (e.g., 1 s). The high mass resolution of the mass detector (approximately 4000–5000) allows isobars to be resolved. A list of mass-to-charge (m/z) ratios of some selected VOCs is shown in Table S1 in the Supplement.

Periodic calibrations of the PTR-ToF-MS were performed on-site for α-pinene, isoprene, methanol, acetone, methyl vinyl ketone (MVK), and 2-methyl-3-buten-2-ol (MBO). Post-campaign calibration of formic acid was obtained utilizing heated perme-ation tubes. The sensitivity of formic acid was then ratioed to the acetone sensitivity measured both during and after the campaign, and the ratio together with the ace-tone field calibration was used to retrieve formic acid from the field measurements. The sensitivities and limits of detection (LOD) of calibrated VOCs are shown in Table S1. Three one-hour integrated VOCs samples were also collected each day in 3 L stainless steel canisters. Analysis for both polar and non-polar compounds was carried out off-site by gas chromatography. It should be noted that the PTR-ToF-MS isoprene signal at m/z 69.070 can be influenced significantly by MBO fragments so that a correction factor based on the linear correlation between the isoprene concentrations determined by PTR-ToF-MS and canister samples (i.e., canister isoprene = 0.7 · PTR-ToF-MS iso-prene, R^2 = 0.79) was used to correct the real-time isoprene concentration measured by the PTR-ToF-MS for the MBO interference.

2.4   Ozone and OH radical measurements

Ozone was measured by a UV absorption monitor (Model TECO 49C, Thermo Envi-ronmental Instruments Inc.). During the last 10 days of the campaign, hydroxyl (OH) radicals were measured using the well-established technique of chemical ionization mass spectrometry (OH-CIMS) (Tanner et al., 1997). The instrument has been previ-

ACPD

15, 28005–28035, 2015

Substantial SOA formation in a coniferous forest

A. K. Y. Lee et al.

Title Page

Abstract	Introduction
Conclusions	References
Tables	Figures

Back | Close

Full Screen / Esc

Printer-friendly Version

Interactive Discussion

ously described (Berresheim et al., 2000; Sjostedt et al., 2007; Tanner et al., 1997). Briefly, hydroxyl radicals are measured by titration with isotopically labelled $^{34}SO_2$ to produce $H^{34}SO_4$. The isotopically labelled sulfuric acid molecules were then ionized by charge transfer with nitrate ions (NO_3^-), produced by passing a flow of nitrogen containing HNO_3 through a ^{210}Po ion source. In order to minimize wall losses of OH radicals, a flow of 2400 standard L min^{-1} is drawn through an inlet with 7.6 cm inner diameter and about 2 feet in length. The instrument background was determined periodically by adding hexafluoropropene (C_3H_6) through the front injectors to scavenge the ambient OH radicals. Calibrations were performed in situ by photolyzing water vapor with a mercury pen ray lamp in the sampling inlet. The detection limit for a 5 min integration of OH radical was 5×10^4 molecules cm^{-3}.

3   Results and discussion

Figure 1 shows the time series of various measurements from 1 to 19 July, which can be divided into three periods based on the meteorological conditions previously reported (Ahlm et al., 2013; Pierce et al., 2012; Macdonald et al., 2015). The first period (1–5 July) was humid and cloudy with low temperature. A relatively high concentration of secondary sulfate indicates that this period was influenced by anthropogenic sources. The second period (6–10 July) started with increasing ambient temperature was accompanied by rapidly increasing levels of biogenic volatile organic compounds (BVOCs, e.g., monoterpenes and isoprene) which were followed by increasing total organic aerosol mass (Fig. 1a–c). This period is referred to as the "biogenic period" hereafter and is the focus of Sects. 3.1 and 3.2. The aerosol sulfate (Fig. 1c) and NO_x mixing ratio (average $\pm$ standard deviation $= 0.4 \pm 0.8$ ppbv) were low during the biogenic period, indicating limited influence by anthropogenic emissions. The third period (13–19 July) was cooler than the biogenic period. Although the diurnal cycles of different measurements indicate that the third period had both biogenic and anthropogenic

Title Page

Abstract | Introduction

Conclusions | References

Tables | Figures

|◀ | ▶|

◀ | ▶

Back | Close

Full Screen / Esc

Printer-friendly Version

Interactive Discussion

influence, the observations provide insights into the pathways of biogenic secondary organic aerosol (BSOA) formation during the biogenic period (Sect. 3.3). The significance of night time nitrate radical chemistry will be discussed in Sect. 3.4. Lastly, a comparison between previous laboratory studies and these field observations will be discussed in Sect. 3.5.

3.1 Biogenic period

Enhancement of BVOC (monoterpenes and isoprene) emissions from the forest due to high temperature and/or solar radiation was observed throughout the campaign (Fig. 1a and b). Specifically, significant positive correlations of daily average temperature and monoterpenes ($R^2 = 0.91$) and isoprene ($R^2 = 0.84$) mixing ratios were obtained (Fig. S3). The forested area in Whistler is dominated by conifers. Therefore, monoterpenes, rather than isoprene, are the dominant BVOCs emitted into air. For example, for the biogenic period, monoterpenes observed at the site were about a factor of three higher than isoprene. Considering the low SOA formation yield from gas-phase isoprene photo-oxidation chemistry determined in smog chamber experiments, monoterpenes likely play a more critical role than isoprene in BSOA formation in Whistler (Lee et al., 2006a, b). Note that sesquiterpenes could not be determined by the PTR-ToF-MS; thus their contributions to BSOA formation cannot be evaluated.

The uniform air mass within the biogenic period led to the accumulation of organic aerosol (Fig. 1c) (Macdonald et al., 2015). The organic aerosols formed during the pristine event were almost entirely biogenic in origin as determined by the FTIR analysis of filter samples during this period (Ahlm et al., 2013). Inorganic constituents generally accounted for less than 5 % of the total NR-PM by mass. Even though the sulfate concentration was slightly enhanced during the strong new particle formation events on 5 and 6 July (i.e., particle number rapidly increased in the 20–30 nm size range), the particle growth to diameters larger than 100 nm was primarily due to condensation of BSOA materials on the nucleation mode particles (Fig. 1c and e) (Pierce et al., 2012). There were strong correlations among methanol, acetone, and SOA throughout

the the study (Figs. 2 and S4). Given that methanol sources are dominated by terrestrial vegetation, correlations between these species throughout the campaign suggest that the observed acetone and SOA were strongly influenced by biogenic sources. The methanol-to-acetone ratio determined in this study is 3.61 ($R^2 = 0.94$). The correlation between total organic aerosol mass and formic acid ($R^2 = 0.77$) is also presented in Fig. S4. Overall, the biogenic episode provides a unique opportunity to investigate the properties and formation mechanisms of BSOA in a forested area dominated by terpene emissions.

3.2 Chemical characteristics of BSOA

Positive matrix factorization (PMF) was performed to understand the chemical characteristics of BSOA. The PMF analysis separates the total organic aerosol into three factors: background organic aerosol (background OA), biogenic SOA-1 (BSOA-1), and biogenic SOA-2 (BSOA-2). The mass spectra and time series of these factors are shown in Figs. 3a–c and 1d, respectively. The background OA represents aged organic aerosol with an intense signal of CO_2^+ fragments (i.e., a tracer of organic acid) and a high degree of oxygenation (O : C = 0.87), and largely correlates with secondary sulfate (see Sect. 3.3). The BSOA-1 and BSOA-2 factors represent two different types of fresh BSOA based on their mass spectral features and temporal profiles (see Sect. 3.3). Elemental analysis shows that the degree of oxygenation of BSOA-2 (O : C = 0.58) and BSOA-1 (O : C = 0.56) was similar even though they have very different m/z 44-to-m/z 43 ratios (a parameter for evaluating the degree of aging of oxygenated OA (OOA) from unit mass resolution AMS spectra) (Ng et al., 2010). Note that the fraction of organic CO_2^+ fragments to the total OA mass (fCO_2^+) reflects the volatility of ambient OA in general (Huffman et al., 2009). A higher values of fCO_2^+ indicates the OA with lower volatility, i.e., OA volatility: BSOA-1 > BSOA-2 > Background OA.

The Van-Krevelen diagram in Fig. 3d shows that the ambient data (orange dots for the biogenic period only) can be a linear combination of the three PMF factors.

The linear fit of ambient data from the whole campaign (slope = −0.35 and y intercept = 1.67) is shown in Fig. 3d. The y-intercept is close to the theoretical H : C of most BVOCs such as isoprene (C_5H_8), α-pinene ($C_{10}H_{16}$), limonene ($C_{10}H_{16}$), and β-caryophyllene ($C_{15}H_{24}$). Furthermore, some major products of α-pinene ozonoylsis including cis-pinonic acid, pinic acid, 3-methyl-1,2,3-butanetricarboxylic acid (MBTCA) fall along the linear fit of the ambient data, consistent with the VOC measurements that terpenes are likely one of the major BSOA precursors in the Whistler forest (see Sect. 3.1). Cis-pinonic and pinic acids are α-pinene first generation products with the average saturation vapor concentrations (C^*) categorized as intermediate-VOCs (IVOCs, $C^* = 10^3$–10^6 $\mu g\,m^{-3}$) and semi-VOCs (SVOCs, $C^* = 10^2$–10^0 $\mu g\,m^{-3}$), respectively (Donahue et al., 2012). MBTCA is a low volatility ($C^* = 10^{-1}$–10^{-3} $\mu g\,m^{-3}$), later generation product of α-pinene SOA and a tracer of terpene SOA. It is important to note that the observed growth for small particles (< 50 nm) at the early stage of the biogenic period in Whistler must have an average C^* less than 10^{-2} $\mu g\,m^{-3}$ based on the modeling results from Pierce et al. (2012). This implies that at least small amounts of organic materials with volatility much lower than BSOA-1 and 2 (e.g., ELVOC observed by Ehn et al., 2014) were required to permit the observed initial growth.

3.3 Understanding BSOA formation from its diurnal character

At the beginning of the biogenic period when there were significant nucleation, BSOA-1 was more prevalent than BSOA-2. BSOA-2, however, sustained the particle growth at the elevated temperature after the new particle formation event on 7 July, likely because of its low volatility. BSOA-1 started to decline from 8 July and the total organic mass was dominated by BSOA-2 during the rest of the biogenic period. The temporal profile of the BSOA-1-to-BSOA-2 ratio is shown in Fig. S6 to illustrate the relative contribution of these BSOA factors within the biogenic period. These observations imply different formation chemistry of the two BSOA materials within the biogenic period (see later discussion).

Substantial SOA formation in a coniferous forest

A. K. Y. Lee et al.

Title Page

Abstract | Introduction

Conclusions | References

Tables | Figures

|◄ | ►|

◄ | ►

Back | Close

Full Screen / Esc

Printer-friendly Version

Interactive Discussion

To gain further insight into the BSOA formation, the diurnal cycles of various measurements were investigated during the period from 13 to 19 July, i.e., during a mix of biogenic and anthropogenic influence. Macdonald et al. (2015) describes the mountain flows during this period which contribute to the diurnal variations in chemistry at the measurement site. The clear diurnal patterns within that period permit evaluation of both the influence of photochemistry and meteorological conditions on the formation of BSOA-1 and BSOA-2. Figure 4a illustrates the morning increase in OH radical concentrations and ozone mixing ratios due to increases in solar radiation (i.e., indicated by the elevated ambient temperature), suggesting more active photo-oxidative chemistry during the daytime and less deposition in the case of ozone. The reaction rate constants of monoterpenes with ozone and OH radical are on the order of 10^{-15}–10^{-17} and 10^{-10}–10^{-11} cm^3 molecule^{-1} s^{-1}, respectively, and both oxidation processes give comparable SOA formation yields for monoterpenes (Lee et al., 2006a, b). Given that the concentrations of ozone and OH radical during the daytime are on the order of 10^{11} and 10^5–10^6 molecules cm^{-3}, respectively (Fig. 4a), the overall contributions of ozonolysis and OH oxidation of monterpenes to daytime BSOA formation in Whistler can be comparable to each other, even though ozonolysis may play a larger role than OH oxidation in late afternoon and night time.

Monoterpene mixing ratios were highest during the night and then dropped rapidly once the concentrations of oxidants built up in the morning (Fig. 4b). Since monoterpene emissions are generally a function of ambient temperature, this observation indicates that monoterpenes are rapidly oxidized due to the presence of OH radical and ozone during the daytime. The increased mixing depth in the morning might also contribute to the drop of the monoterpene mixing ratios. In contrast, other BVOCs and their oxidation products such as acetone, isoprene and probably MVK/methacrolein (MACR; PTR-ToF-MS cannot separate MVK and MACR, and other isoprene oxidation products may contribute to this mass-to-charge ratio signal) increased in connection with ozone, providing further evidence of active photochemistry during the day. The similar diurnal cycles of these VOCs were also clearly observed during the later period of the biogenic

episode (i.e. 9–10 July, Fig. 1). Different diurnal cycles of isoprene and monoterpene mixing ratios were observed previously in forest (Harrison et al., 2001). Note that isoprene emission flux is sensitive to both solar radiation and temperature (Rinne et al., 2002).

The diurnal variations of background OA and secondary sulfate are almost identical (Fig. 4c), and their concentrations peak at around 17:00 LT due to the upslope winds that carry anthropogenic/aged aerosol particles to the sampling site (Macdonald et al., 2015). The background OA can be successfully separated from the BSOA components using the PMF analysis. Comparing the total OA, the BSOA components, and the background OA, it is clear that the total organic mass within the biogenic period was not strongly influenced by anthropogenic sources and/or transported air masses (Fig. 1d). The BSOA-2 diurnal profile matches the variation of ozone plus OH radical levels during the daytime, suggesting that oxidation of monoterpenes and its oxidation products is likely one of the major BSOA-2 formation pathways. Note that the isoprene SOA signature (i.e. a high mass fraction of m/z 82 to total organic mass, f82) was not observed in the mass spectrum of BSOA-2 (Fig. 3c).

BSOA-1 has a diurnal pattern clearly distinct from BSOA-2, with a night time peak. BSOA-1 is likely more volatile than BSOA-2 based on their relative $f\mathrm{CO}_2^+$ values, as shown in Fig. 3. The low temperature at night thus favours partitioning of BSOA-1 materials to the particle phase, resulting in a higher concentration of BSOA-1 at night. In addition to the gas-particle partitioning of BSOA-1 materials, BSOA-1 formation via ozonolysis of monoterpenes at night is also possible because of the large abundance of monoterpenes and presence of ozone. Lastly, BSOA-2 was composed of a higher fraction of organic acids (i.e., $f\mathrm{CO}_2^+$) compared to BSOA-1. Additional information is required to evaluate the possibility of heterogeneous conversion of BSOA-1 to BSOA-2 during the daytime (see Sect. 3.5).

3.4 Nitrate radical chemistry at night

Nitrate radical ($NO_3\cdot$) is a product of ozone and NO_x and is a well-known nocturnal oxidant. Xu et al. (2015) recently reported that $NO_3\cdot$ chemistry could play a key role in producing BSOA at night in southeast United States. The average ozone and NO_x mixing ratios at night during WACS 2010 were about 20–30 ppbv (Fig. 4) and 0.34 ppbv (Fig. 5a and c) throughout the entire study, respectively, which are comparable to the levels reported by Xu et al. (2015) (i.e. $O_3 = 21$ ppbv and $NO_x = 0.54$ ppbv). Laboratory studies have shown that organic nitrates can be produced from the reaction between $NO_3\cdot$ and BVOCs (Ng et al., 2008; Fry et al., 2009). It has been shown that fragmentation of organic nitrates produces NO^+ and NO_2^+ signal in AMS measurement with the NO^+/NO_2^+ ratio much higher than that of inorganic nitrate (e.g. Framer et al., 2010). The NO^+/NO_2^+ ratio of ammonium nitrate determined in our calibration was approximately 3.38. In contrast, the average NO^+/NO_2^+ ratio observed in the AMS measurement was 9.6 and it was relatively constant throughout the sampling period. The diurnal cycle of ambient NO^+/NO_2^+ ratio between 13 and 19 July is shown in Fig. 5c. The high values of NO^+/NO_2^+ ratio indicate low levels of inorganic nitrate and the presence of organic nitrates in the observed BSOA (e.g. Framer et al., 2010; Xu et al., 2015).

No diurnal cycles of NO^+ and NO_2^+ AMS fragments were observed (Fig. S7) to confirm significant $NO_3\cdot$ chemistry at night, possibly due to the upslope mixing of anthropogenic/aged aerosol particles mentioned in the previous sections. There was some covariance in the temporal variations of sulfate and nitrate (Fig. S8). To evaluate the possibility of night time $NO_3\cdot$ chemistry in this study, the AMS nitrate mass is normalized by sulfate mass to eliminate the potential effects of upslope mixing on nitrate aerosol concentrations. The NO_3^-/SO_4^{2-} ratio correlates extremely well with the BSOA-1 ($R^2 = 0.71$) for the whole sampling period (Fig. 5b). Furthermore, the diurnal pattern of this ratio during the later period (13–18 July) was almost identical to that of BSOA-1 (Fig. 5d), indicating the formation of organic nitrates at night. The formation of organic nitrates during the biogenic episode under relatively high temperature and low RH con-

Full Screen / Esc

Printer-friendly Version

Interactive Discussion

ditions further suggests that the diurnal cycle of the NO_3^-/SO_4^{2-} ratio cannot be fully explained by gas-particle partitioning of nitric acid which would occur preferentially at lower temperatures.

Assuming the NO^+/SO_4 and NO_2^+/SO_4 mass ratios were constant in the air mass carried by upslope winds and are approximately equal to 0.088 and 0.009 respectively (i.e. the minimum values observed during the upslope wind condition), the NO^+ and NO_2^+ mass originating from the upslope wind air masses can be subtracted from their total mass loadings. After that, the mass loading of nitrate functional groups (-ONO_2) in organic compounds and thus the organic nitrate mass contributing to the observed BSOA-1 mass can be estimated using the calculation approach used by Xu et al. (2015) (see details in the Supplement) and assuming the molecular weight of the organic nitrates to be 200–300 $g\,mol^{-1}$. The organic nitrate mass accounted for 22–33 % of BSOA-1 at night and its diurnal cycle (ranged from 0.05 to 0.2 $\mu g\,m^{-3}$) is shown in Fig. 5d. Results of these calculations suggest that organic nitrates can be a significant contributor to BSOA mass produced via night time $NO_3\cdot$ chemistry. Similarly, Xu et al. (2015) estimated that the organic nitrates accounted for 40–60 % of less oxidized OOA (LO-OOA) mass observed during the night time.

3.5 Comparison to previous laboratory studies

Formation pathways of BSOA can also potentially be evaluated through examination of specific mass fragments. The organic fragment at m/z 91 has been commonly observed in the laboratory-generated and ambient BSOA and in this study both BSOA-1 and BSOA-2 factors have a distinct peak at m/z 91, mostly due to the presence of the $C_7H_7^+$ fragment (Fig. 3). Even though the mass fraction of m/z 91 to total organic (f91) is not a unique indicator for BSOA (Ng et al., 2011), it can be potentially used to evaluate the formation pathways of BSOA in this unpolluted, biogenic-rich environment (e.g., identify potential BSOA precursors, evaluate relative importance of gas-phase and heterogeneous chemistry).

The f91 values of both raw data and PMF results are shown in Fig. 6a along with f91 values from previously-published laboratory and field measurements. The BSOA-1 and BSOA-2 factors determined in this study are much higher than the f91 for α-pinene SOA generated in smog chamber experiments at low NO_x condition with a comparable organic loading ($\sim 6\,\mu g\,cm^{-3}$) (Chen et al., 2015). In contrast, SOA generated from β-caryophyllene (a sesquiterpene) can produce values of f91 comparable to that of our ambient data (Chen et al., 2015). Previous plant chamber experiments (i.e. oxidation of a mixture of BVOCs) also suggest that the value of f91 likely depends on the relative contribution of sesquiterpenes to total BVOCs; the average value of f91 of SOA generated by the oxidation of different plant emissions is reported here (Kiendler-Scharr et al., 2009). Note that a boreal forest study in Finland also observed a high value of f91 using PMF analysis (Finessi et al., 2012). The above comparisons indicate that in addition to monoterpenes, sesquiterpenes may have contributed to the BSOA formation in Whistler.

Laboratory studies have also shown that some of the first generation products of α-pinene ozonolysis can have a high level of f91 in their AMS spectra. For example, cis-pinonic acid droplets generated by atomization (Lee et al., 2012) and pinonaldehyde uptake to sulfuric acid particles (Liggio and Li, 2006) give high f91 values. Although cis-pinonic acid and pinonaldehyde are rather volatile, they may experience significant wall loss in smog chambers during the SOA formation experiments previously reported (Mueller et al., 2012; Zhang et al., 2015). Therefore, the wall effect can suppress subsequent gas-phase reactions of intermediate products that may produce less volatile, SOA-forming organic acids with the same f91 signature. Since the surface characteristics of the land and vegetation in the remote forested region can be very different to the wall surface of smog chambers, it is possible that α-pinene ozonolysis can also be an important source of the $C_7H_7^+$ fragments in the real atmosphere.

The difference in the f91 values between BSOA-1 and BSOA-2 can be further used to evaluate the relationship between these two PMF factors. In the same campaign at Whistler, Slowik et al. (2012) performed a set of in-situ heterogeneous OH oxidation

Title Page

Abstract | Introduction

Conclusions | References

Tables | Figures

|◀ | ▶|

◀ | ▶

Back | Close

Full Screen / Esc

Printer-friendly Version

Interactive Discussion

experiments using a flow tube reactor to age BSOA sampled during the biogenic period. They clearly observed that the f91 value declined with heterogeneous oxidation and the mass spectra of reaction products determined by PMF analysis did not contain a high value of f91. Because BSOA-2 has a higher level of f91 than BSOA-1 (Fig. 6), we conclude that there is little heterogeneous oxidative conversion of BSOA-1 to BSOA-2.

4   Conclusions and atmospheric implications

The strong biogenic episode observed in this study provides a unique opportunity to improve current understanding of BSOA formation chemistry in a coniferous forest. The high levels of SOA formation are comparable to those previously observed in the summertime in another Canadian forested location also dominated by terpene emissions (Slowik et al., 2010). Given the considerably emphasis placed on isoprene SOA in the past few years and given the high SOA levels observed in this study, there is merit to addressing also the formation of SOA in these coniferous forested regions. Indeed, with pronounced high latitude warming it is very important to better understand SOA formation in such regions to know how they will respond to changing climate conditions (Leaitch et al., 2011).

The BSOA observed during the biogenic episode was primarily due to ozonolysis and OH oxidation of BVOCs (i.e., monoterpenes and perhaps sesquiterpenes) during the day. We also provide evidence that nitrate radical chemistry with BVOCs at night can be significant. PMF analysis identified two types of BSOA, namely BSOA-1 and BSOA-2, and separated them from the background organic aerosol. BSOA-1 represents gas-phase ozonolysis and nitrate radical oxidation products, and is likely semi-volatile in nature, resulting in higher concentrations at low ambient temperature during the night. BSOA-2 has a much stronger CO_2^+ signal (i.e. a lower vapor pressure) than BSOA-1, and consists of products from gas-phase oxidation by OH radical and ozone during the day. Hence, the temporal variations of BSOA-1 and BSOA-2 observed here are due to their gas-particle partitioning in response to ambient temperature, the relative

importance of different oxidation chemistry between day and night, and the gradual oxidation of early generation gas-phase oxidation products. The calculation in Sect. 3.4 suggests that BSOA-1 can be largely contributed by organic nitrates at night (22–33 % by mass) due to nitrate radical chemistry.

This study evaluates the values of f91 obtained from the AMS measurements as a tracer to investigate the BSOA-2 potential formation pathways. Although sesquiterpenes (e.g., β-caryophyllene) can be important precursors to generate SOA with high f91 values, the average plant chamber SOA (i.e., a mixture of BVOCs including isoprene, monoterpenes, and sesquiterpenes) better represents the characteristics (f43, f44 and f91) of BSOA-1 than BSOA-2, as shown in Fig. 6. We also demonstrated that heterogeneous oxidation of BSOA-1 is expected to be a minor production pathway of BSOA-2. Nevertheless, we cannot rule out the possibility that some BSOA-1 material repartitions to the gas phase due to elevated temperature during the daytime and then undergoes gas-phase oxidation to produce BSOA-2 materials. This may partly explain the decay of BSOA-1 and a higher level of BSOA-2 observed in the later period of biogenic episode.

Our observations highlight the potential importance of gas-phase formation chemistry of BSOA-2 type materials (i.e. relatively high f91 and f44) that have not been captured in laboratory experiments, perhaps due to the wall loss of gas-phase intermediate products. For example, cis-pinonic acid is the first generation product of α-pinene ozonolysis that can have significant wall loss in the chamber (Mueller et al., 2012). The wall effects may suppress gas-phase reactions of such intermediate products that may produce SOA with high values of f44 and f91 (i.e. organic acids with f91 signature). Zhang et al. (2015) recently reported the wall deposition rate of 25 oxidized organic compounds generated from the photo-oxidation of various SOA precursors in Teflon chambers. Furthermore, Zhang et al. (2014) showed that the losses of organic vapors to chamber walls during photooxidation of toluene can lead to substantial underestimation of SOA yields.

References

Ahlm, L., Shakya, K. M., Russell, L. M., Schroder, J. C., Wong, J. P. S., Sjostedt, S. J., Hayden, K. L., Liggio, J., Wentzell, J. J. B., Wiebe, H. A., Mihele, C., Leaitch, W. R., and Macdonald, A. M.: Temperature-dependent accumulation mode particle and cloud nuclei concentrations from biogenic sources during WACS 2010, Atmos. Chem. Phys., 13, 3393–3407, doi:10.5194/acp-13-3393-2013, 2013.

Aiken, A. C., Decarlo, P. F., Kroll, J. H., Worsnop, D. R., Huffman, J. A., Docherty, K. S., Ulbrich, I. M., Mohr, C., Kimmel, J. R., Sueper, D., Sun, Y., Zhang, Q., Trimborn, A., Northway, M., Ziemann, P. J., Canagaratna, M. R., Onasch, T. B., Alfarra, M. R., Prevot, A. S. H., Dommen, J., Duplissy, J., Metzger, A., Baltensperger, U., and Jimenez, J. L.: O/C and OM/OC ratios of primary, secondary, and ambient organic aerosols with high-resolution time-of-flight aerosol mass spectrometry, Environ. Sci. Technol., 42, 4478–4485, 2008.

Allan, J., Delia, A., Coe, H., Bower, K., Alfarra, M., Jimenez, J., Middlebrook, A., Drewnick, F., Onasch, T., Canagaratna, M., Jayne, J., and Worsnop, D.: A generalised method for the extraction of chemically resolved mass spectra from aerodyne aerosol mass spectrometer data, J. Aerosol Sci., 35, 909–922, 2004.

Berresheim, H., Elste, T., Plass-Dulmer, C., Eisele, F. L., and Tanner, D. J.: Chemical ionization mass spectrometer for long-term measurements of atmospheric OH and H_2SO_4, Int. J. Mass Spectrom., 202, 91–109, 2000.

Blake, R. S., Monks, P. S., and Ellis, A. M.: Proton-transfer reaction mass spectrometry, Chem. Rev., 109, 861–896, 2009.

Substantial SOA formation in a coniferous forest

A. K. Y. Lee et al.

Title Page

Abstract	Introduction
Conclusions	References
Tables	Figures

◀ | ▶◀
◀ | ▶

Back | Close

Full Screen / Esc

Printer-friendly Version

Interactive Discussion

Canagaratna, M. R., Jimenez, J. L., Kroll, J. H., Chen, Q., Kessler, S. H., Massoli, P., Hilde-
brandt Ruiz, L., Fortner, E., Williams, L. R., Wilson, K. R., Surratt, J. D., Donahue, N. M.,
Jayne, J. T., and Worsnop, D. R.: Elemental ratio measurements of organic compounds using
aerosol mass spectrometry: characterization, improved calibration, and implications, Atmos.
Chem. Phys., 15, 253–272, doi:10.5194/acp-15-253-2015, 2015.

Chen, Q., Farmer, D. K., Schneider, J., Zorn, S. R., Heald, C. L., Karl, T. G., Guenther, A.,
Allan, J. D., Robinson, N., Coe, H., Kimmel, J. R., Pauliquevis, T., Borrmann, S., Poeschl, U.,
Andreae, M. O., Artaxo, P., Jimenez, J. L., and Martin, S. T.: Mass spectral characterization of
submicron biogenic organic particles in the Amazon Basin, Geophys. Res. Lett., 36, L20806,
doi:10.1029/2009GL039880, 2009.

Chen, Q., Farmer, D. K., Rizzo, L. V., Pauliquevis, T., Kuwata, M., Karl, T. G., Guenther, A.,
Allan, J. D., Coe, H., Andreae, M. O., Pöschl, U., Jimenez, J. L., Artaxo, P., and Martin, S. T.:
Submicron particle mass concentrations and sources in the Amazonian wet season (AMAZE-
08), Atmos. Chem. Phys., 15, 3687–3701, doi:10.5194/acp-15-3687-2015, 2015.

Chhabra, P. S., Flagan, R. C., and Seinfeld, J. H.: Elemental analysis of chamber organic
aerosol using an aerodyne high-resolution aerosol mass spectrometer, Atmos. Chem. Phys.,
10, 4111–4131, doi:10.5194/acp-10-4111-2010, 2010.

de Gouw, J. and Warneke, C.: Measurements of volatile organic compounds in the earths
atmosphere using proton-transfer-reaction mass spectrometry, Mass Spectrom. Rev., 26,
223–257, 2007.

DeCarlo, P. F., Kimmel, J. R., Trimborn, A., Northway, M. J., Jayne, J. T., Aiken, A. C., Go-
nin, M., Fuhrer, K., Horvath, T., Docherty, K. S., Worsnop, D. R., and Jimenez, J. L.:
Field-deployable, high-resolution, time-of-flight aerosol mass spectrometer, Anal. Chem., 78,
8281–8289, 2006.

Ehn, M., Kleist, E., Junninen, H., Petäjä, T., Lönn, G., Schobesberger, S., Dal Maso, M., Trim-
born, A., Kulmala, M., Worsnop, D. R., Wahner, A., Wildt, J., and Mentel, Th. F.: Gas phase
formation of extremely oxidized pinene reaction products in chamber and ambient air, Atmos.
Chem. Phys., 12, 5113–5127, doi:10.5194/acp-12-5113-2012, 2012.

Ehn, M., Thornton, J. A., Kleist, E., Sipila, M., Junninen, H., Pullinen, I., Springer, M.,
Rubach, F., Tillmann, R., Lee, B., Lopez-Hilfiker, F., Andres, S., Acir, I., Rissanen, M.,
Jokinen, T., Schobesberger, S., Kangasluoma, J., Kontkanen, J., Nieminen, T., Kurten, T.,
Nielsen, L. B., Jorgensen, S., Kjaergaard, H. G., Canagaratna, M., Dal Maso, M.,
Berndt, T., Petaja, T., Wahner, A., Kerminen, V., Kulmala, M., Worsnop, D. R., Wildt, J.,

and Mentel, T. F.: A large source of low-volatility secondary organic aerosol, Nature, 506, 476–479, doi:10.1038/nature13032, 2014.

Farmer, D. K., Matsunaga, A., Docherty, K. S., Surratt, J. D., Seinfeld, J. H., Ziemann, P. J., and Jimenez, J. L.: Response of an aerosol mass spectrometer to organonitrates and organosulfates and implications for atmospheric chemistry, P. Natl. Acad. Sci. USA, 107, 6670–6675, 2010.

Finessi, E., Decesari, S., Paglione, M., Giulianelli, L., Carbone, C., Gilardoni, S., Fuzzi, S., Saarikoski, S., Raatikainen, T., Hillamo, R., Allan, J., Mentel, Th. F., Tiitta, P., Laaksonen, A., Petäjä, T., Kulmala, M., Worsnop, D. R., and Facchini, M. C.: Determination of the biogenic secondary organic aerosol fraction in the boreal forest by NMR spectroscopy, Atmos. Chem. Phys., 12, 941–959, doi:10.5194/acp-12-941-2012, 2012.

Fry, J. L., Kiendler-Scharr, A., Rollins, A. W., Wooldridge, P. J., Brown, S. S., Fuchs, H., Dubé, W., Mensah, A., dal Maso, M., Tillmann, R., Dorn, H.-P., Brauers, T., and Cohen, R. C.: Organic nitrate and secondary organic aerosol yield from NO_3 oxidation of β-pinene evaluated using a gas-phase kinetics/aerosol partitioning model, Atmos. Chem. Phys., 9, 1431–1449, doi:10.5194/acp-9-1431-2009, 2009.

Goldstein, A. H., Koven, C. D., Heald, C. L., and Fung, I. Y.: Biogenic carbon and anthropogenic pollutants combine to form a cooling haze over the southeastern United States, P. Natl. Acad. Sci. USA, 106, 8835–8840, 2009.

Han, Y., Iwamoto, Y., Nakayama, T., Kawamura, K., and Mochida, M.: Formation and evolution of biogenic secondary organic aerosol over a forest site in Japan, J. Geophys. Res.-Atmos., 119, 259–273, 2014.

Harrison, D., Hunter, M. C., Lewis, A. C., Seakins, P. W., Bonsang, B., Gros, V., Kanakidou, M., Touaty, M., Kavouras, I., Mihalopoulos, N., Stephanou, E., Alves, C., Nunes, T., and Pio, C.: Ambient isoprene and monoterpene concentrations in a Greek fir (*Abies Borisii-regis*) forest. Reconciliation with emissions measurements and effects on measured OH concentrations, Atmos. Environ., 35, 4699–4711, 2001.

Huffman, J. A., Docherty, K. S., Aiken, A. C., Cubison, M. J., Ulbrich, I. M., DeCarlo, P. F., Sueper, D., Jayne, J. T., Worsnop, D. R., Ziemann, P. J., and Jimenez, J. L.: Chemically-resolved aerosol volatility measurements from two megacity field studies, Atmos. Chem. Phys., 9, 7161–7182, doi:10.5194/acp-9-7161-2009, 2009.

Kanakidou, M., Seinfeld, J. H., Pandis, S. N., Barnes, I., Dentener, F. J., Facchini, M. C., Van Dingenen, R., Ervens, B., Nenes, A., Nielsen, C. J., Swietlicki, E., Putaud, J. P., Balkan-

Title Page

Abstract | Introduction

Conclusions | References

Tables | Figures

|◀ | ▶|

◀ | ▶

Back | Close

Full Screen / Esc

Printer-friendly Version

Interactive Discussion

ski, Y., Fuzzi, S., Horth, J., Moortgat, G. K., Winterhalter, R., Myhre, C. E. L., Tsigaridis, K., Vignati, E., Stephanou, E. G., and Wilson, J.: Organic aerosol and global climate modelling: a review, Atmos. Chem. Phys., 5, 1053–1123, doi:10.5194/acp-5-1053-2005, 2005.

Kiendler-Scharr, A., Zhang, Q., Hohaus, T., Kleist, E., Mensah, A., Mentel, T. F., Spindler, C., Uerlings, R., Tillmann, R., and Wildt, J.: Aerosol mass spectrometric features of biogenic SOA: observations from a plant chamber and in rural atmospheric environments, Environ. Sci. Technol., 43, 8166–8172, 2009.

Leaitch, W. R., Macdonald, A. M., Brickell, P. C., Liggio, J., Sjostedt, S. J., Vlasenko, A., Bottenheim, J. W., Huang, L., Li, S.-M., Liu, P. S. K., Toom-Sauntry, D., Hayden, K. A., Sharma, S., Shantz, N. C., Wiebe, H. A., Zhang, W., Abbatt, J. P. D., Slowik, J. G., Chang, R. Y. W., Russell, L. M., Schwartz, R. E., Takahama, S., Jayne, J. T., and Ng, N. L.: Temperature response of the submicron organic aerosol from temperate forests, Atmos. Environ., 45, 6696–6704, doi:10.1016/j.atmosenv.2011.08.047, 2011.

Lee, A., Goldstein, A. H., Keywood, M. D., Gao, S., Varutbangkul, V., Bahreini, R., Ng, N. L., Flagan, R. C., and Seinfeld, J. H.: Gas-phase products and secondary aerosol yields from the ozonolysis of ten different terpenes, J. Geophys. Res.-Atmos., 111, D07302, doi:10.1029/2005JD006437, 2006a.

Lee, A., Goldstein, A. H., Kroll, J. H., Ng, N. L., Varutbangkul, V., Flagan, R. C., and Seinfeld, J. H.: Gas-phase products and secondary aerosol yields from the photooxidation of 16 different terpenes, J. Geophys. Res.-Atmos., 111, D17305, doi:10.1029/2006JD007050, 2006b.

Lee, A. K. Y., Hayden, K. L., Herckes, P., Leaitch, W. R., Liggio, J., Macdonald, A. M., and Abbatt, J. P. D.: Characterization of aerosol and cloud water at a mountain site during WACS 2010: secondary organic aerosol formation through oxidative cloud processing, Atmos. Chem. Phys., 12, 7103–7116, doi:10.5194/acp-12-7103-2012, 2012.

Liggio, J. and Li, S.: Reactive uptake of pinonaldehyde on acidic aerosols, J. Geophys. Res.-Atmos., 111, D24303, doi:10.1029/2005JD006978, 2006.

Macdonald, A. M., Leaitch, W. R., Abbatt, J. P. D., Ahlm, L., Al-Basheer, W., Betram, A. K., Buller, J., Campuzano-Jost, P., Chan, E., Corbin, J., Cziczo, D., Elford, A., Hayden, K. A., Herckes, P., Lee, A. K. Y., Li, S.-M., Liggio, J., Liu, P. S. K., Mihele, C., Noone, K. J., Pierce, J. R., Russell, L. M., Toom-Sauntry, D., Schroder, J., Sharma, S., Sheppard, A., Sjostedt, S. J., Slowik, J. G., Strawbridge, K., Stupple, G., Vlasenko, A., Wainwright, C., Wang, Y.,

Wentzell, J., Wiebe, H. A., and Wong, J. P. S.: An overview of the 2010 WACS2010: biogenic aerosol formation, mountain flows and CCN, in preparation, 2015.

Martin, S. T., Andreae, M. O., Althausen, D., Artaxo, P., Baars, H., Borrmann, S., Chen, Q., Farmer, D. K., Guenther, A., Gunthe, S. S., Jimenez, J. L., Karl, T., Longo, K., Manzi, A., Müller, T., Pauliquevis, T., Petters, M. D., Prenni, A. J., Pöschl, U., Rizzo, L. V., Schneider, J., Smith, J. N., Swietlicki, E., Tota, J., Wang, J., Wiedensohler, A., and Zorn, S. R.: An overview of the Amazonian Aerosol Characterization Experiment 2008 (AMAZE-08), Atmos. Chem. Phys., 10, 11415–11438, doi:10.5194/acp-10-11415-2010, 2010.

Müller, L., Reinnig, M.-C., Naumann, K. H., Saathoff, H., Mentel, T. F., Donahue, N. M., and Hoffmann, T.: Formation of 3-methyl-1,2,3-butanetricarboxylic acid via gas phase oxidation of pinonic acid – a mass spectrometric study of SOA aging, Atmos. Chem. Phys., 12, 1483–1496, doi:10.5194/acp-12-1483-2012, 2012.

Ng, N. L., Kwan, A. J., Surratt, J. D., Chan, A. W. H., Chhabra, P. S., Sorooshian, A., Pye, H. O. T., Crounse, J. D., Wennberg, P. O., Flagan, R. C., and Seinfeld, J. H.: Secondary organic aerosol (SOA) formation from reaction of isoprene with nitrate radicals (NO_3), Atmos. Chem. Phys., 8, 4117–4140, doi:10.5194/acp-8-4117-2008, 2008.

Ng, N. L., Canagaratna, M. R., Zhang, Q., Jimenez, J. L., Tian, J., Ulbrich, I. M., Kroll, J. H., Docherty, K. S., Chhabra, P. S., Bahreini, R., Murphy, S. M., Seinfeld, J. H., Hildebrandt, L., Donahue, N. M., DeCarlo, P. F., Lanz, V. A., Prévôt, A. S. H., Dinar, E., Rudich, Y., and Worsnop, D. R.: Organic aerosol components observed in Northern Hemispheric datasets from Aerosol Mass Spectrometry, Atmos. Chem. Phys., 10, 4625–4641, doi:10.5194/acp-10-4625-2010, 2010.

Ng, N. L., Canagaratna, M. R., Jimenez, J. L., Zhang, Q., Ulbrich, I. M., and Worsnop, D. R.: Real-time methods for estimating organic component mass concentrations from aerosol mass spectrometer data, Environ. Sci. Technol., 45, 910–916, 2011.

Pierce, J. R., Leaitch, W. R., Liggio, J., Westervelt, D. M., Wainwright, C. D., Abbatt, J. P. D., Ahlm, L., Al-Basheer, W., Cziczo, D. J., Hayden, K. L., Lee, A. K. Y., Li, S.-M., Russell, L. M., Sjostedt, S. J., Strawbridge, K. B., Travis, M., Vlasenko, A., Wentzell, J. J. B., Wiebe, H. A., Wong, J. P. S., and Macdonald, A. M.: Nucleation and condensational growth to CCN sizes during a sustained pristine biogenic SOA event in a forested mountain valley, Atmos. Chem. Phys., 12, 3147–3163, doi:10.5194/acp-12-3147-2012, 2012.

Title Page

Abstract | Introduction

Conclusions | References

Tables | Figures

|◄ | ►|

◄ | ►

Back | Close

Full Screen / Esc

Printer-friendly Version

Interactive Discussion

Rinne, H., Guenther, A., Greenberg, J., and Harley, P.: Isoprene and monoterpene fluxes measured above Amazonian rainforest and their dependence on light and temperature, Atmos. Environ., 36, 2421–2426, 2002.

Seinfeld, J. H. and Pandis, S. N.: Atmospheric Chemistry and Physics: from Air Pollution to Climate Change, 2nd Edn., J. Wiley, New York, 2006.

Setyan, A., Zhang, Q., Merkel, M., Knighton, W. B., Sun, Y., Song, C., Shilling, J. E., Onasch, T. B., Herndon, S. C., Worsnop, D. R., Fast, J. D., Zaveri, R. A., Berg, L. K., Wiedensohler, A., Flowers, B. A., Dubey, M. K., and Subramanian, R.: Characterization of submicron particles influenced by mixed biogenic and anthropogenic emissions using high-resolution aerosol mass spectrometry: results from CARES, Atmos. Chem. Phys., 12, 8131–8156, doi:10.5194/acp-12-8131-2012, 2012.

Shilling, J. E., Chen, Q., King, S. M., Rosenoern, T., Kroll, J. H., Worsnop, D. R., DeCarlo, P. F., Aiken, A. C., Sueper, D., Jimenez, J. L., and Martin, S. T.: Loading-dependent elemental composition of α-pinene SOA particles, Atmos. Chem. Phys., 9, 771–782, doi:10.5194/acp-9-771-2009, 2009.

Shilling, J. E., Zaveri, R. A., Fast, J. D., Kleinman, L., Alexander, M. L., Canagaratna, M. R., Fortner, E., Hubbe, J. M., Jayne, J. T., Sedlacek, A., Setyan, A., Springston, S., Worsnop, D. R., and Zhang, Q.: Enhanced SOA formation from mixed anthropogenic and biogenic emissions during the CARES campaign, Atmos. Chem. Phys., 13, 2091–2113, doi:10.5194/acp-13-2091-2013, 2013.

Sjostedt, S. J., Huey, L. G., Tanner, D. J., Peischl, J., Chen, G., Dibb, J. E., Lefer, B., Hutterli, M. A., Beyersdorf, A. J., Blake, N. J., Blake, D. R., Sueper, D., Ryerson, T., Burkhart, J., and Stohl, A.: Observations of hydroxyl and the sum of peroxy radicals at Summit, Greenland during summer 2003, Atmos. Environ., 41, 5122–5137, 2007.

Slowik, J. G., Stroud, C., Bottenheim, J. W., Brickell, P. C., Chang, R. Y.-W., Liggio, J., Makar, P. A., Martin, R. V., Moran, M. D., Shantz, N. C., Sjostedt, S. J., van Donkelaar, A., Vlasenko, A., Wiebe, H. A., Xia, A. G., Zhang, J., Leaitch, W. R., and Abbatt, J. P. D.: Characterization of a large biogenic secondary organic aerosol event from eastern Canadian forests, Atmos. Chem. Phys., 10, 2825–2845, doi:10.5194/acp-10-2825-2010, 2010.

Slowik, J. G., Wong, J. P. S., and Abbatt, J. P. D.: Real-time, controlled OH-initiated oxidation of biogenic secondary organic aerosol, Atmos. Chem. Phys., 12, 9775–9790, doi:10.5194/acp-12-9775-2012, 2012.

Substantial SOA formation in a coniferous forest

A. K. Y. Lee et al.

Title Page

Abstract	Introduction
Conclusions	References
Tables	Figures

Back | Close

Full Screen / Esc

Printer-friendly Version
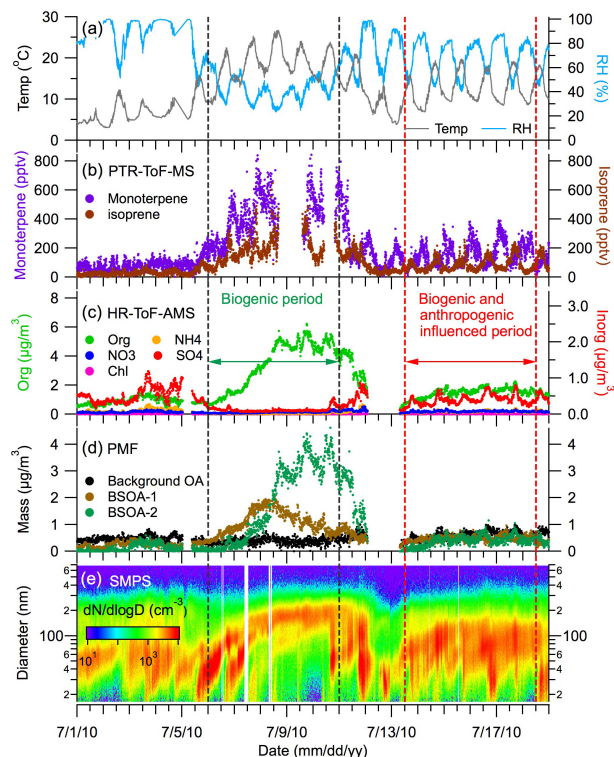
Interactive Discussion

Tanner, D. J., Jefferson, A., and Eisele, F. L.: Selected ion chemical ionization mass spectrometric measurement of OH, J. Geophys. Res.-Atmos., 102, 6415–6425, 1997.

Ulbrich, I. M., Canagaratna, M. R., Zhang, Q., Worsnop, D. R., and Jimenez, J. L.: Interpretation of organic components from Positive Matrix Factorization of aerosol mass spectrometric data, Atmos. Chem. Phys., 9, 2891–2918, doi:10.5194/acp-9-2891-2009, 2009.

Xu, L., Guo, H., Boyd, C. M., Klein, M., Bougiatioti, A., Cerully, K. M., Hite, J. R., Isaacman-VanWertz, G., Kreisberg, N. M., Knote, C., Olson, K., Koss, A., Goldstein, A. H., Hering, S. V., de Gouw, J., Baumann, K., Lee, S., Nenes, A., Weber, R. J., and Ng, N. L.: Effects of anthropogenic emissions on aerosol formation from isoprene and monoterpenes in the southeastern United States, P. Natl. Acad. Sci. USA, 112, 37–42, 2015.

Zhang, X., Cappa, C. D., Jathar, S. H., McVay, R. C., Ensberg, J. J., Kleeman, M. J., and Seinfeld, J. H.: Influence of vapor wall loss in laboratory chambers on yields of secondary organic aerosol, P. Natl. Acad. Sci. USA, 111, 5802–5807, 2014.

Zhang, X., Schwantes, R. H., McVay, R. C., Lignell, H., Coggon, M. M., Flagan, R. C., and Seinfeld, J. H.: Vapor wall deposition in Teflon chambers, Atmos. Chem. Phys., 15, 4197–4214, doi:10.5194/acp-15-4197-2015, 2015.

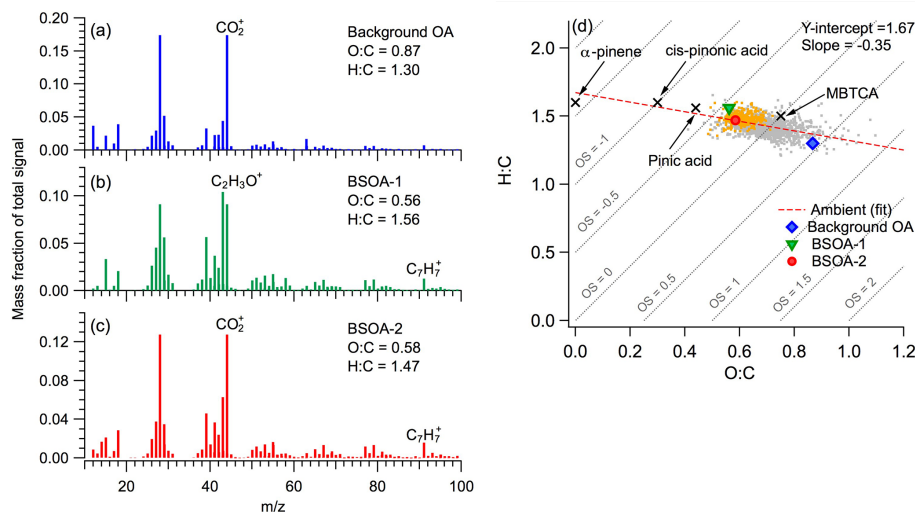Title Page

Abstract | Introduction

Conclusions | References

Tables | Figures

|◀ | ▶|

◀ | ▶

Back | Close

Full Screen / Esc

Printer-friendly Version

Interactive Discussion

Figure 1. Time series (PST) profiles of **(a)** temperature and relative humidity, **(b)** monoterpene and isoprene measured by PTR-ToF-MS, **(c)** organic, nitrate, sulfate, ammonium, and chloride measured by HR-ToF-AMS, **(d)** background OA, BSOA-1, and BSOA-2 determined by PMF analysis, **(e)** particle number size distribution measured SMPS. The gray and red dashed lines represent the boundaries of the biogenic period (6–10 July) and the period with a mix of biogenic and anthropogenic influences (13–18 July), respectively. Figure S2 enlarges the time series during **(a)** 6–10 July and **(b)** 13–18 July.

Discussion Paper | Discussion Paper | Discussion Paper | Discussion Paper |

Title Page

Abstract | Introduction

Conclusions | References

Tables | Figures

|◄ | ►|

◄ | ►

Back | Close

Full Screen / Esc

Printer-friendly Version

Interactive Discussion
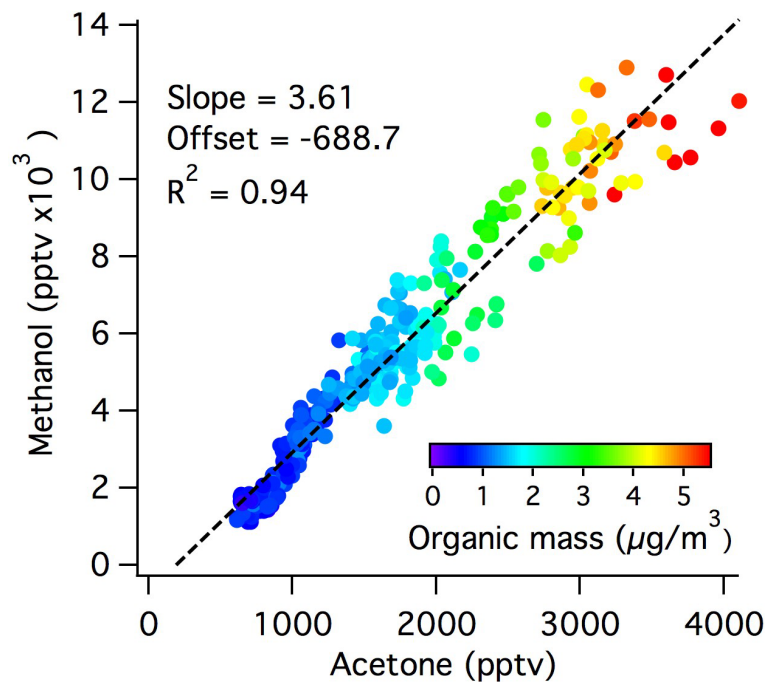
Figure 2. Correlation of methanol and acetone measured by PTR-ToF-MS. The color scales represent the total organic mass measured by HR-ToF-AMS.

Title Page

Abstract | Introduction

Conclusions | References

Tables | Figures

|◄ | ►|

◄ | ►

Back | Close

Full Screen / Esc

Printer-friendly Version

Interactive Discussion

Figure 3. Normalized unit mass resolution mass spectra of PMF factors **(a)** background OA, **(b)** BSOA-1, and **(c)** BSOA-2. **(d)** Van-Krevelen diagram: orange and gray dots represent observations from the regional biogenic period (6–10 July) and the whole study period, respectively. The cross symbols represent the $O:C$ and $H:C$ ratios of α-pinene and its major oxidation products (cis-pinonic acid, pinic acid, 3-methyl-1,2,3-butanetricarboxylic acid (MBTCA)). The histograms of $O:C$ and $H:C$ distributions are shown in Fig. S5.
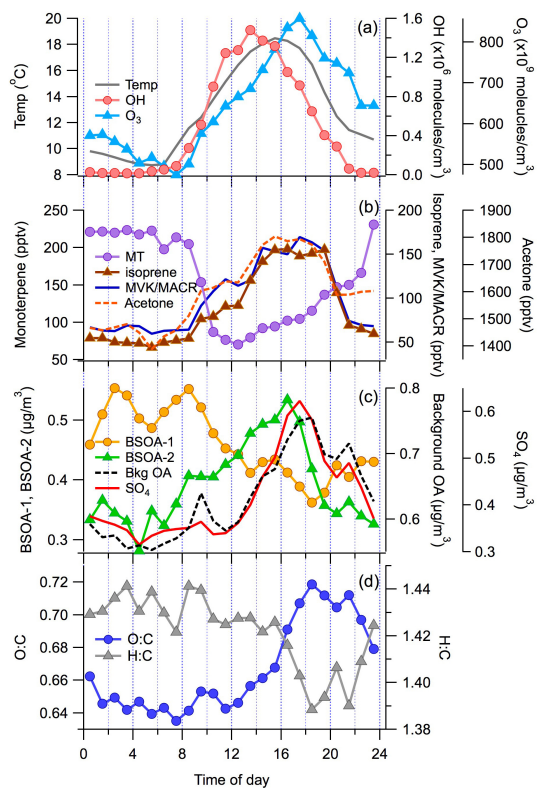
Figure 4. Diurnal cycles of **(a)** temperature, OH radical and ozone **(b)** monoterpene (MT), isoprene, methyl vinyl ketone (MVK)/methacrolein (MACR), and acetone, **(c)** background OA, BSOA-1, BSOA-2 and SO_4, and **(d)** elemental compositions of total organics (O : C and H : C) observed during 13–18 July. Note that the OH radical concentration is the average value measured after 19 July.

Title Page

Abstract | Introduction

Conclusions | References

Tables | Figures

|◄ | ►|

◄ | ►

Back | Close

Full Screen / Esc

Printer-friendly Version

Interactive Discussion
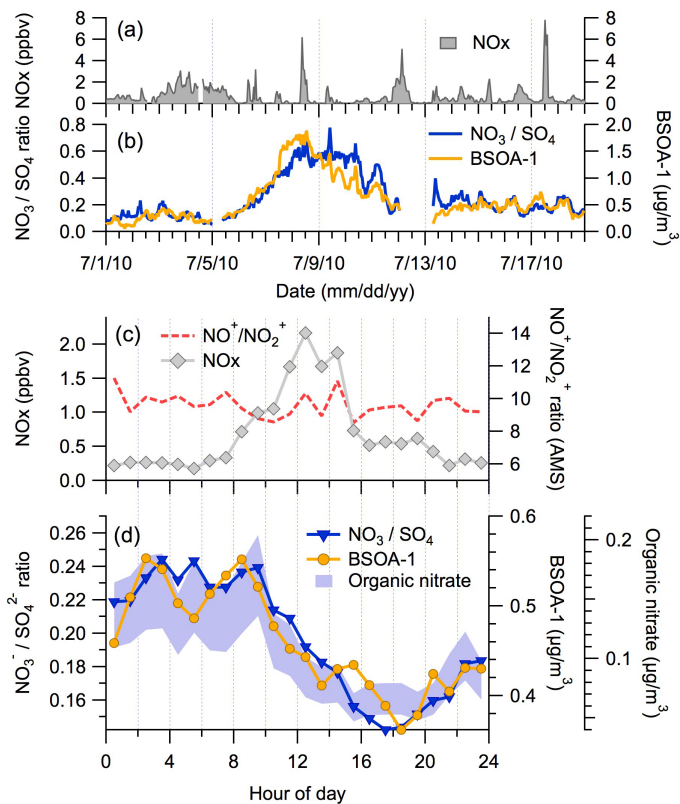
Figure 5. Time series (PST) profiles of **(a)** NO_x mixing ratio and **(b)** NO_3^-/SO_4^{2-} ratio and mass loading of BSOA-1. Diurnal cycles of **(c)** NO_x mixing ratio and NO^+/NO_2^+ ratio measured by HR-ToF-AMS and **(d)** NO_3^-/SO_4^{2-} ratio and mass loadings of BSOA-1 and organic nitrates.
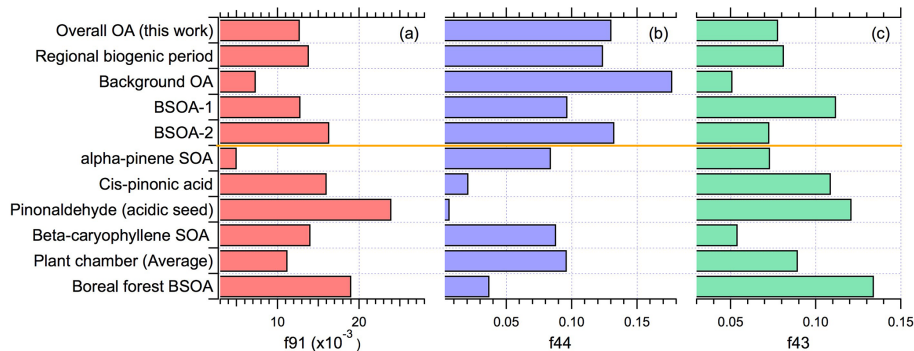
Figure 6. The mass fraction of **(a)** m/z 91 (f91), **(b)** m/z 44 (f44), and **(c)** m/z 43 (f43) observed in this study (overall OA, regional biogenic period, background OA, BSOA-1 and BSOA-2), α-pinene and β-caryophyllene SOA generated by chamber experiments (Chen et al., 2015), pinonaldehyde uptake on sulphuric acid seeds (Liggio and Li, 2006), plant chamber SOA (Kiendler-Scharr et al., 2009), cis-pinonic acid (Lee et al., 2012), and BSOA observed in boreal forest in Finland (Finessi et al., 2012).